On-site camera calibration with sub-block of images for UAS Photogrammetry corridor mapping with on-board GNSS-RTK

Kalima Pitombeira [1], Edson Mitishita [1], Charles Toth [2], Marcelo de Abreu [3]

[1] Geomatics Department, Federal University of Paraná, Curitiba, PR, Brazil – kalimapitombeira@ufpr.br, mitishita@ufpr.br
[2] Dept. of Civil, Environmental and Geodetic Engineering, The Ohio State University, Columbus, OH, USA – toth.2@osu.edu
[3] Tecsystem Company, Castelo, ES, Brazil – marcelo@imaginair.com.br

Keywords: *In-situ* camera calibration, On-the-job camera calibration, GNSS-Assisted Aerial Triangulation, Interior Orientation Parameters, Structure from Motion – Multi-view Stereo.

Abstract

UAS photogrammetry has gained popularity due to its efficiency and automation in acquiring spatial data. Among its applications, corridor mapping is essential for road and railway planning, transmission line inspection, coastal monitoring, and river geomorphological analysis. High spatial accuracy in corridor mapping typically requires dense GCP distribution or precise sensor position and orientation measurements. When using the direct sensor position obtained by GNSS-RTK, camera calibration is essential in reducing vertical bias on the photogrammetric intersection. Although previous studies have demonstrated the benefits of incorporating multi-height oblique images for improving vertical accuracy, there is a lack of research on more feasible data acquisition strategies for corridor mapping, such as using sub-blocks of oblique images for calibration. Thus, this study addresses this gap by evaluating the impact of different sub-block configurations on IOP estimation and spatial data accuracy. The results show that incorporating oblique images into on-site calibrations significantly improves IOP estimation, particularly for focal length, compared to an on-the-job calibration with only nadir images. Vertical accuracy improves by up to 79% in GNSS-AAT experiments using oblique images, making it possible to achieve checkpoint RMSEs for each coordinate (X, Y, and Z) of approximately 1 GSD, without the need for GCPs. In contrast, on-the-job calibration with nadir images alone resulted in higher Z-axis errors. These findings suggest that using nadir and oblique sub-blocks for on-site calibration can improve vertical accuracy, reduce reliance on GCPs in corridor mapping, and maintain high spatial accuracy.

1. Introduction

Unmanned Aerial Systems (UAS) have gained significant popularity over the past decade as a platform for aerial photogrammetry, primarily due to their ease of use, the development of consumer-grade sensors, and the automation of flight paths and remote-control operations (Liu *et al*., 2022). Simultaneously, advancements in photogrammetry, computer vision, and digital image processing have contributed to the widespread adoption of the Structure from Motion – Multi-view Stereo (SfM-MVS) workflow within the geospatial community, enabling high levels of automation for spatial data acquisition (Deliry and Avdan, 2021).

Compared to manned aircraft, UAS imagery is typically captured at low above-ground-level (AGL) altitudes, resulting in characteristics similar to terrestrial close-range photogrammetry, such as higher perspective distortions and significant variations in scale and lighting within a single survey. Due to robust feature descriptors such as SIFT (Lowe, 2004) and SURF (Bay *et al*., 2008), SfM - MVS performs well to obtain a dense point cloud, even under varying conditions of light, scale, and rotation of images, while maintaining a high degree of automation (Smith *et al*., 2016). As a result, the SfM-MVS workflow performs well with UAS photogrammetry for robust 3D information extraction (Eltner *et al*., 2015).

UAS Photogrammetry for corridor mapping has great potential to enable surveys along linear features, improving the cost-effectiveness of applications such as road and railway mapping (Ferrer-González *et al*., 2020), transmission line inspection, coastal region monitoring (Nahon et al., 2019), and river geomorphological studies (La Salandra *et al*., 2023). Corridor surveys can be distinguished by the dimensions of the image block where the length along the flight direction is significantly greater than the width, resulting in a block with, usually, one or two long flight strips. To ensure high-accuracy spatial data acquisition under these geometric conditions, a high degree of forward and side overlap and the use of numerous Ground Control Points (GCPs) are required.

However, conducting field surveys for GCP can be hazardous in certain situations, such as floods, landslides, or wildfires, or costly in areas with difficult access, such as dense vegetation, glacial terrain, or mountainous regions (Antoine *et al*., 2020). Therefore, reducing or eliminating the need for GCPs is desirable.

To reduce the number of Ground Control Points required in a photogrammetric survey, the camera's position and orientation can be measured using on-board sensors such as a Global Navigation Satellite System (GNSS) receiver and Inertial Navigation System (INS) (Przybilla *et al*., 2020). Unfortunately, consumer-grade UAS typically do not include high-resolution INS for orientation measurement mainly because of the high cost associated with accurate INS and UAS payload limitations (Gonçalves and Henriques, 2015). Conversely, modern UAS equipped with high-precision on-board GNSS receivers have become more common, enabling the computation of sensor position during flight using Real-Time Kinematic (RTK) or Post-Processed Kinematic (PPK) (Stöcker *et al*., 2017). In this context, the camera station coordinates can be constrained as additional observations in the Bundle Adjustment – BA, refining the position and orientation of the images' block, i.e., GNSS-Assisted Aerial Triangulation (GNSS-AAT) or GNSS-Assisted Integrated Sensor Orientation (Benjamin *et al*., 2020).

In indirect georeferencing of images (BA), minor inaccuracies in camera calibration parameters (Interior Orientation Parameters - IOPs) can be partially absorbed by the estimation of the camera's position and orientation (Exterior Orientation Parameters – EOPs) due to the direct correlation between some IOP with EOP parameters; thereby minimizing the impact of IOP inaccuracies on the spatial acquisition accuracy (Mitishita *et al.*, 2014). In contrast, in direct georeferencing of images, where the EOPs are fixed, inaccuracies of the IOPs are propagated to the 3D coordinates of points, causing a more significant effect on the accuracy of geo-information extraction (Habib *et al*., 2010). From this perspective, accurate camera calibration (accurate IOPs) can ensure high positional quality when using direct georeferencing of images.

In UAS photogrammetry, off-the-shelf digital cameras are generally less stable than metric cameras, leading to more significant variability in camera calibration parameters under different flight conditions, such as temperature fluctuations, minor vibrations, and landing impacts (Cledat *et al*., 2020). On-the-job calibration (or self-calibration) is widely used for UAS imagery (Forlani *et al*., 2018); in this methodology, the IOPs are estimated within the same bundle adjustment used for spatial data acquisition (i.e., 3D points triangulation/intersection). In this approach, some interior orientation parameters, under flight conditions, can model the atmospheric refraction, fixing the collinearity condition model. On the other hand, some IOP estimations can model other unintended effects that deviate from the collinearity condition, introducing bias into the IOP estimation and consequently affecting the accuracy of geo-information extraction. Several strategies can help reduce the correlation among these parameters during camera calibration, such as conducting flights at different heights above ground level - AGL, employing cross-strip flight patterns, incorporating oblique images, and using direct measurements of sensor position and orientation (LUHMANN *et al*., 2006).

In corridor mapping, due to the block's geometry with long flight strips, it is not always viable to conduct multiple flights along the entire corridor (Andaru *et al.*, 2020). Consequently, relying solely on vertical images at the same flight height can result in high correlations between IOPs and EOPs when performing on-the-job calibration (Zhou *et al*., 2019). As an alternative, previous studies have demonstrated that sub-blocks of images can be used for camera calibrations, helping to reduce the need for GCPs in photogrammetric surveys, both in manned aircraft (Costa *et al*. 2018) and UAS imagery (Pitombeira and Mitishita, 2023) with traditional Photogrammetry workflow.

However, to our knowledge, there is a lack of studies investigating image sub-blocks for camera calibration in UAS photogrammetry using SfM-MVS and sensor position during flight. This approach could provide a more feasible method for incorporating multiple flight heights and oblique images in corridor mapping, thereby enhancing geoinformation extraction without needing Ground Control Points (GCPs). In this context, the present study aims to address this gap by estimating IOP values with on-site camera calibrations using various image sub-block configurations (including oblique images and different flight heights) to acquire spatial data for corridor mapping using UAS GNSS-AAT without relying on GCPs.

2. Related Work

Zhou *et al.* (2019) assessed the influence of camera calibration errors on UAS photogrammetric mapping over a 200 m x 30 m corridor, using a synthetic error-free dataset to simulate different scenarios. Errors were manually introduced to the focal length, and the erroneous calibrations were established as initial solutions in the BA. The experiments combining nadir and oblique images or nadir images at multiple flight heights enable accurate re-estimation of erroneous focal length during bundle adjustment. However, vertical drift in camera poses occurs when fixing the IOPs from the erroneous calibrations (i.e., without performing camera re-calibration), to compensate for focal length errors and improve 3D measurement accuracy. On the other hand, in scenarios where introduced errors in focal length values vary gradually during the survey (simulating temperature fluctuations), multi-height vertical images do not yield significant improvements. However, including oblique and vertical images has shown the potential to reduce the drift on camera position estimation and, thus, increase the accuracy of 3D geo-information extraction.

Meinen and Robinson (2020) investigated the use of UAS corridor mapping for streambank topography analysis on seven banks within three study sites. A comparison between the UAS-SFM pipeline and a terrestrial laser scanner benchmark revealed that UAS-derived models presented an average 3D Root Mean Square Error (RMSE) of about 4 GSD using 14 to 16 GCPs per study site. The study found significant variations in IOP estimation through self-calibration across UAS surveys conducted on different banks. These variations were mainly observed in lens radial distortion coefficients, indicating inaccurate camera calibration and resulting in non-linear errors in the point clouds, known as the doming effect (James and Robson, 2014).

Ferrer-González et al. (2020) analyzed the distribution of ground control points (GCPs) along a 2.1 km x 190 m road corridor block of vertical images. Four different GCP distributions were investigated, each with varying numbers of points, resulting in a total of 13 configurations. Based on the experiments, for achieving horizontal RMSE of 3 GSD, five or more GCPs were necessary, while for vertical RMSE of 5 GSD, seven or more GCPs. Although the authors acknowledge the importance of well-estimated camera calibration on corridor mapping accuracy, on-the-job calibration was performed in all experiments without further discussion of variations in IOP values. In that sense, the checkpoint accuracies, mainly on vertical RMSE, highlight that estimating EOPs by indirect sensor orientation and, simultaneously, IOP by on-the-job calibration requires high GCP density to achieve relatable spatial data acquisition in corridor mapping.

Pilartes-Congo *et al*. (2024) evaluated UAS-SfM and UAS-Lidar survey repeatability of a roadway surface on a 460 m x 25 m corridor, using direct sensor positions obtained by on-board GNSS-PPK receiver. Two nadir flights were conducted with UAS imagery for the Digital Terrain Model – DTM generation, both processed without GCP and with 4 GCPs. The two photogrammetric experiments without GCP presented a vertical bias on the checkpoint’s accuracies, leading to an RMSE Z value of 6-8 GSD. Adding 4 GCPs significantly improved the geo-information extraction, leading to checkpoint’s RMSE Z of 1-2 GSD. These results show that even using directly measured camera coordinates as constraints, performing on-the-job calibration only with nadir images may lead to noticeable bias on the model elevation, which could be caused by imprecisions in IOP estimation. Therefore, the study outcomes support that adding GCP is essential to obtaining a high-accuracy corridor block DTM when using GNSS-AAT with single-height nadir images.

Andaru *et al.,* (2022) proposed a camera calibration pipeline and a co-registration method using UAS SfM photogrammetry for sandbank morphological monitoring through multi-temporal

https://doi.org/10.5194/isprs-annals-X-G-2025-657-2025

images along a 30 km x 1 km corridor. Two datasets (one test field and one on-site) were used for camera calibration named by the authors as "semi-on-the-job-self-calibration". The first step consisted of using the test-field data set (with cross-strips flight lines, multi-heigh vertical images, and directly measured camera position) and the on-site dataset (with parallel flight lines, single-heigh vertical images, and directly measured camera position) to perform camera calibrations. In the second step, on-the-job calibration experiments were conducted using different combinations of calibrated IOPs as initial parameters. Among all the calibration experiments performed, using the on-site calibration parameters (focal length and principal point coordinates) as fixed and estimating the remaining parameters (lens distortions and affinity) by on-the-job calibration presents the best results of vertical RMSE on checkpoints. Therefore, on-site camera calibration reveals great potential to improve spatial data acquisition quality on corridor mapping when using non-metric cameras on consumer-grade UAS. However, even using GNSS-PPK to measure direct camera position, their results still rely on several GCPs at each data set to assure high accuracy geospatial data.

As discussed in the related work, using UAS Photogrammetry for corridor mapping requires high-density GCP configuration for 3D information extraction with high precision. When an optimal GCP geometric distribution is not available, using camera coordinates obtained by an on-board GNSS receiver can improve spatial data acquisition positional quality, but usually is insufficient to ensure reliable vertical accuracy. In that sense, camera calibration can reduce vertical bias in corridor mapping. Different image acquisition patterns, such as oblique images, cross-strips, and multiple flight heights can substantially improve the precision of IOP estimation. On the one hand, these flight patterns can be easily conducted on a test field; however, due to the instability of non-metric cameras, the internal orientation can change under different survey conditions (e.g. temperature variation, slight vibrations, collisions during landing). Thus, conducting a test-field camera calibration can lead to IOP values that incorrectly model the sensor's physical conditions during the surveys. On the other hand, performing an on-the-job calibration with ideal image acquisition (oblique images, cross-strips, and multiple flight heights) can be a challenge in corridor mapping, mainly because the block geometry composed of long strips makes it difficult to carry on multiple flights along the entire area.

In that context, the current study aims to evaluate a more feasible alternative to applying different flight patterns for camera calibration on corridor mapping to improve IOP estimation precision by using sub-blocks of images. For that goal, experiments of on-site (*in situ*) calibration using sub-blocks of images were performed, including nadir, oblique, and multi-heigh image sub-blocks. From one standpoint, the on-site calibration allows IOP estimation to be conducted in conditions as similar as possible to the full corridor block survey. Furthermore, with the use of image sub-block configurations, the calibration can be carried out on a more controlled and smaller dataset.

3. Methodology

3.1 Study Site

All coordinates in this study are provided in meters and refer to UTM Zone 24S (Geodetic Reference System for the Americas 2000 - SIRGAS 2000). The study site is situated in Cachoeiro de Itapemirim, Espírito Santo, in southeastern Brazil (Figure 1), with centroid coordinates at 20°41'23"S and 41°12'12" W (SIRGAS 2000). This area is located in a countryside (non-urban) region, with elevations varying from 64 to 180 m due to hilly terrain features. The corridor survey of 3.2 km × 450 m encompasses a section of ES-166 state highway, with 225 m on each side of the road axis, and covers an area of approximately 138 ha.

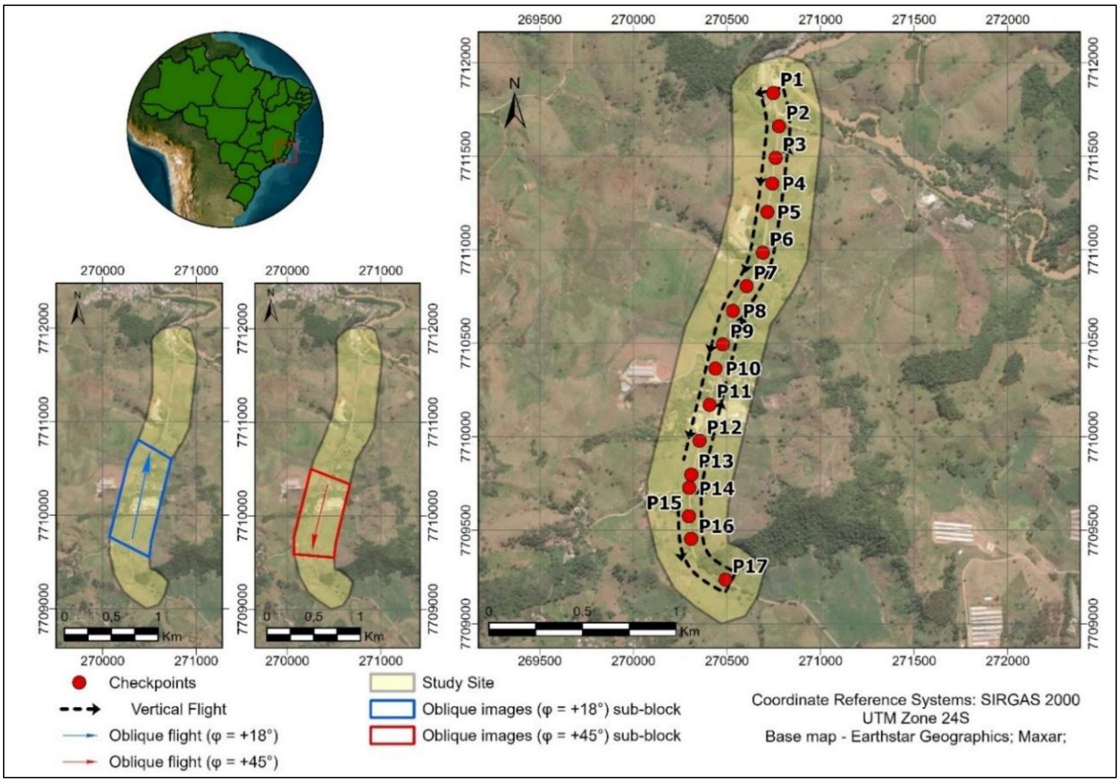

Figure 1. Study site and data acquisition settings

3.2 Data Acquisition

For this study, the DJI Matrice 350 RTK was used for image acquisition, which is a vertical take-off and landing multi-rotor UAS with a maximum flight time of 55 minutes. The UAS was equipped with a DJI Zenmuse P1 camera which has: a sensor size of 35.9 mm x 24 mm, an image size of 8192 x 5460 pixels, a pixel size of 4.39 μm, a global mechanical shutter, and a nominal focal length of 35 mm.

The aerial survey was conducted in three different flight configurations. The first survey included a block with 279 vertical (nadir) images obtained by two parallel strips (one in N-S direction and the other from S-N), with 80% forward overlap and 60% side overlap, taken at a flight height above ground level - AGL of 320 meters, resulting in an average Ground Sample Distance - GSD of 3.8 cm/pixel. Additionally, two sub-blocks of oblique images were acquired at a 200 meters flight height AGL, where: the first had 19 images with an 18° inclination on pitch ($\varphi = +18°$), covering an area of 1.5 ha and 870 m along the road axis; the second had 21 images with a 45° inclination on pitch ($\varphi = +45°$), covering an area of 2.7 ha and 870 m along the road axis.

Before the UAS flights, a field survey was conducted on 17 targets across the study site to serve as checkpoints. For this purpose, two Topcon GNSS RTK receivers (base station and rover), model Hiper SR, were used, with a nominal horizontal accuracy of 10 mm + 0.8 ppm and a nominal vertical accuracy of 15 mm + 1.0 ppm. The height distribution of the targets varies by 30 m, with the northern points at lower elevations, where P1 is the lowest at 70 m, and the southern points at higher elevations, with P15 being the highest at 100 m.

The distribution of checkpoints was established along both sides of the road, resulting in a greater density near the center line of the corridor block. This arrangement was performed due to the focus of the corridor mapping on the road itself and the challenging access to surrounding areas, primarily due to dense vegetation and hilly terrain.

3.3 Photogrammetric Data Processing

The photogrammetric experiments were carried out with the Structure from Motion – Multi-View Stereo (SfM-MVS) pipeline implemented in the commercial product Agisoft Metashape Professional version 2.1.2. The tie point extraction and matching were performed autonomously using images upscaled by a factor of 4 (*Highest* accuracy setting on Metashape). In the bundle adjustment, the tie points observations precisions were established as one pixel (4.39 μm) for x and y image coordinates.

For all the experiments, the camera station coordinates (X_S, Y_S, Z_S) obtained by the on-board GNSS-RTK were used as additional observations on the bundle adjustment and constrained by the RTK survey accuracy for each image (average RMSE of X_S: 0.012 m; Y_S: 0.013 m; Z_S: 0.037 m). Camera orientation angles (ω, φ, κ) were set as unknown to be estimated by the BA.

According to Metashape’s user manual (Agisoft, 2024) the program uses Brown's distortion model to compute the interior orientation of the sensor. For performing the camera calibrations in this study, the following parameters were estimated: focal length (c), principal point coordinates (x_P, y_P), radial symmetric distortion coefficients (k_1, k_2, k_3), and decentering distortion coefficients (p_1, p_2).

3.3.1 On-the-job Camera Calibration

Initially, one experiment of on-the-job camera calibration (OTJCalib) was performed using the corridor block with 279 vertical (nadir) images acquired at a 320 meters flight height AGL. That experiment was carried out to compare the estimated IOP values with the on-site camera calibrations proposed in this study. Furthermore, this experiment was also conducted to investigate the accuracy of geo-information extraction by on-the-job camera calibration without GCPs and with 17 checkpoints. The image-space coordinates of the checkpoints were manually measured using a monocular view, enabling the photogrammetric intersection to compute their 3D object-space coordinates.

3.3.2 On-situ Camera Calibration

To analyze IOP estimation by camera calibration, four on-site calibrations (OSCalib) were performed with different sub-block configurations, presented in Table 1.

The image sub-block for all calibrations was established in the central-southern area of the corridor block, as shown in Figure 1.

3.3.3 GNSS-Assisted Aerial Triangulation

According to Table 2, four experiments of GNSS-AAT were conducted to investigate the influence of on-site calibration with different sub-block configurations on the spatial data acquisition accuracy.

The GNSS-AAT experiments were conducted using the same sub-block of oblique images included in the corresponding on-site calibration. In this context, the subsequent analyses can assess the impact of incorporating each oblique sub-block configuration throughout the entire photogrammetric process, i.e., on the calibration step and on the 3D geo-information extraction.

All the GNSS-AAT experiments were performed without GCPs, thus, the 17 targets surveyed were used as checkpoints. The image-space coordinates of checkpoints were measured manually by monocular view.

3.3.4 Accuracy Assessment

The RMSE values of checkpoint discrepancies, i.e., the RMSE of the differences between the 3D coordinates surveyed by RTK (ground truth) and those estimated by photogrammetric intersection, were used to evaluate the accuracy of the five spatial data acquisition experiments: one on-the-job calibration (OTJCalib) and four GNSS-AAT experiments.

The checkpoint discrepancies were also computed to highlight possible bias in the 3D coordinates (X, Y, Z).

4. Results

4.1 Camera Calibration

Table 3 presents the values of the Interior Orientation Parameters (IOPs) and their respective precision, estimated from the on-the-job calibration and the four on-site camera calibration experiments conducted in this study.

Analyzing the Interior Orientation Parameters (IOPs) estimated from the four on-site calibration experiments with different sub-block configurations reveals that the values exhibit no significant variations. The most notable difference is in the focal length (c) estimation between OSCalib_1 and OSCalib_3/OSCalib_4, with a discrepancy of 0.007 mm (1.6 pix). Additionally, as expected, including oblique image sub-blocks in the on-site calibration experiments improves the IOP estimation precision, probably due to increasing scale information along the Z-axis (viewing direction) for the bundle adjustment. The results show that the focal length estimation precision improves by 58x between OSCalib_1 and OSCalib_4. However, the IOP values remain consistent across all the calibrations with image sub-blocks.

	Vertical images corridor block		Oblique images sub-block (φ = +18°)		Oblique images sub-block (φ = +45°)	
	Images	Flight height AGL	Images	Flight height AGL	Images	Flight height AGL
OSCalib_1	40	320 m	-	-	-	-
OSCalib_2	40	320 m	19	200 m	-	-
OSCalib_3	40	320 m	-	-	21	200 m
OSCalib_4	40	320 m	19	200 m	21	200 m

Table 1. Details of the on-situ camera calibration experiments performed.

	Vertical images corridor block		Oblique images sub-block (φ = +18°)		Oblique images sub-block (φ = +45°)	
	Images	Flight height AGL	Images	Flight height AGL	Images	Flight height AGL
GNSS_AAT_1	279	320 m	-	-	-	-
GNSS_AAT_2	279	320 m	19	200 m	-	-
GNSS_AAT_3	279	320 m	-	-	21	200 m
GNSS_AAT_4	279	320 m	19	200 m	21	200 m

Table 2. Details of the GNSS-Assisted Aerial Triangulation experiments performed.

IOPs	OTJCalib		OSCalib_1		OSCalib_2		OSCalib_3		OSCalib_4	
	Value	Precision	Value	Precision	Value	Precision	Value	Precision	Value	Precision
c (mm)	35.990	2.02E-03	35.977	1.05E-02	35.972	3.25E-04	35.970	2.72E-04	35.970	1.80E-04
x_P (mm)	-0.134	8.34E-05	-0.133	2.50E-04	-0.134	2.06E-04	-0.134	2.33E-04	-0.134	1.98E-04
y_P (mm)	0.200	1.19E-04	0.197	5.27E-04	0.198	2.28E-04	0.198	2.63E-04	0.199	2.24E-04
k_1 (mm^{-2})	-2.26E-04	6.59E-08	-2.24E-04	2.24E-07	-2.23E-04	1.49E-07	-2.23E-04	1.58E-07	-2.23E-04	1.40E-07
k_2 (mm^{-4})	7.95E-05	3.82E-07	6.55E-05	1.05E-06	6.15E-05	9.22E-07	6.46E-05	9.66E-07	6.25E-05	8.78E-07
k_3 (mm^{-6})	-4.60E-04	7.02E-07	-4.30E-04	2.11E-06	-4.25E-04	1.71E-06	-4.26E-04	1.80E-06	-4.25E-04	1.58E-06
p_1 (mm^{-2})	-3.90E-06	2.68E-09	-3.85E-06	8.34E-09	-3.84E-06	6.59E-09	-3.87E-06	7.46E-09	-3.85E-06	6.59E-09
p_2 (mm^{-2})	1.12E-05	3.60E-09	1.12E-05	1.10E-08	1.12E-05	8.78E-09	1.12E-05	1.10E-08	1.12E-05	8.78E-09

Table 3. IOP values and their precisions obtained in the camera calibration experiments.

On the other hand, when comparing the on-the-job calibration (OTJCalib) using the complete corridor block with nadir images to the on-site calibrations with image sub-blocks (OSCalib 1 to 4), Table 3 reveals a significant variation in focal length, with differences of up to 0.020 mm (4.6 pix) between OTJCalib and OSCalib_3/OSCalib_4, and in the radial distortion parameter k_2, with a variation of up to 22% (1.8E-05 mm^{-4}) between OTJCalib and OSCalib_2.

Another noteworthy result can be observed when comparing the on-the-job calibration (OTJCalib) with the on-site calibration (OSCalib_1). In both experiments, only nadir images were used to compute the IOPs. Therefore, the focal length variation of 0.013 mm (3 pixels) can be attributed to the difference between using the complete corridor block (279 nadir images) and the sub-block (40 nadir images).

For all the calibration experiments, the reprojection error of tie point observations in image-space presented similar values: 0.212 pixels for OTJCalib, 0.208 pixels for OSCalib_1, 0.227 pixels for OSCalib_2, 0.214 pixels for OSCalib_3, and 0.227 pixels for OSCalib_4. Therefore, these results indicate that the calibrations did not result in significant differences in tie point residuals.

4.2 Spatial Data Acquisition Accuracy

To investigate the influence of different camera calibrations on the spatial accuracy of corridor mapping without Ground Control Points, one on-the-job calibration experiment and four GNSS-Assisted Aerial Triangulation experiments, each using different configurations of on-site camera calibrations, were conducted.

Figures 2, 3, and 4 show the checkpoint discrepancies in the on-the-job calibration (OTJCalib) and the four GNSS-AAT experiments, respectively for the coordinates X, Y, and Z.

Analyzing the discrepancies in the X checkpoints 'coordinates across all experiments, a bias along the corridor axis can be highlighted. Checkpoints in the northern section show positive discrepancies, which gradually decrease as the checkpoints approach the central region, where the errors are close to zero. The discrepancies then shift to negative values in the southern portion of the corridor. These results suggest a rotation in the flight azimuth due to imprecisions in estimating the camera stations' orientation angles around the Z-axis (i.e., the kappa/yaw angles). Furthermore, the GNSS-ATT_1 experiment exhibits the most significant errors on X at both ends of the corridor, with a maximum discrepancy of 0.167 m and a minimum of -0.124 m.

https://doi.org/10.5194/isprs-annals-X-G-2025-657-2025 | © Author(s) 2025. CC BY 4.0 License.

The discrepancies in the Y coordinates are more evenly distributed along the corridor axis, however, a noticeable positive bias is present. All the experiments had similar results with slight variation among their Y coordinate discrepancies, with a maximum discrepancy of 0.055 m (OTJCalib) and a minimum of 0.014 m (GNSS-AAT_3).

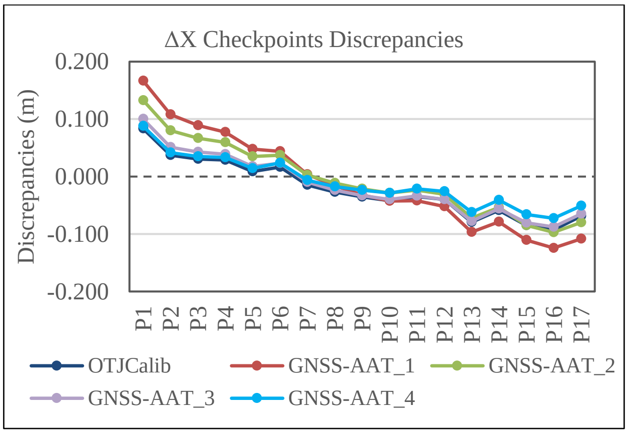

Figure 2. Discrepancies at checkpoints on the X-axis.

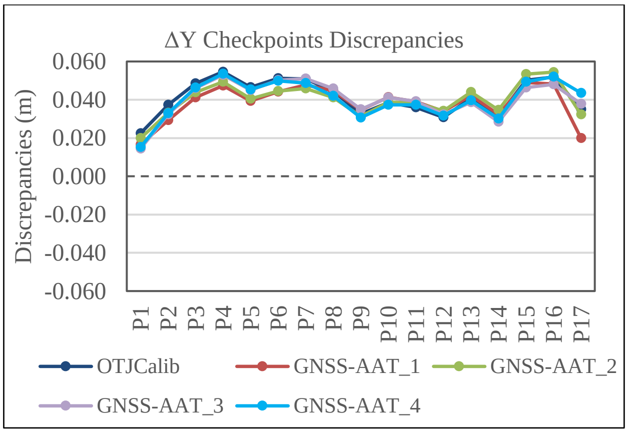

Figure 3. Discrepancies at checkpoints on the Y axis.

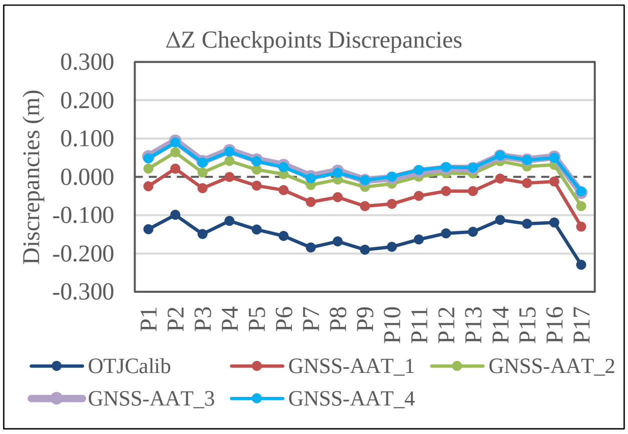

Figure 4. Discrepancies at checkpoints on the Z axis.

Discrepancies in the Z coordinate of the checkpoints show a consistent error pattern along the corridor in all experiments. However, a significant negative bias is observed in experiments without oblique images, particularly in the OTJCalib using the corridor block of 279 nadir images, where discrepancies range from -0.099 m to -0.230 m. These results may be attributed to the focal length estimation, as shown in Table 3: the two experiments with bigger focal length values (OTJCalib and GNSS-ATT_1) resulted in the most significant bias in the Z checkpoints discrepancies.

Figure 5 presents the Root Mean Square Error (RMSE) for X, Y, and Z checkpoint discrepancies, as well as for the horizontal (XY) and tridimensional (XYZ) components, aiming to show the accuracies obtained in the calibration experiments more succinctly.

When comparing the on-the-job calibration experiment with a block of 279 vertical images (OTJCalib) to the on-site calibration with a sub-block of 40 vertical images (GNSS-AAT_1), a significant reduction in the RMSE for the Z coordinate is observed, decreasing from 0.154 m to 0.051 m, representing a 67% improvement in vertical accuracy. However, as shown in Figures 2 and 5, a bias in the X-axis emerged in the GNSS-AAT_1 experiment, leading to an increase in horizontal RMSE from 0.068 m in OTJCalib to 0.093 m in GNSS-AAT_1. Despite this, the vertical error in OTJCalib significantly impacts the overall 3D error (0.168 m), which was improved by 37% in GNSS-AAT_1 (0.106 m), as reflected in the RMSE XYZ.

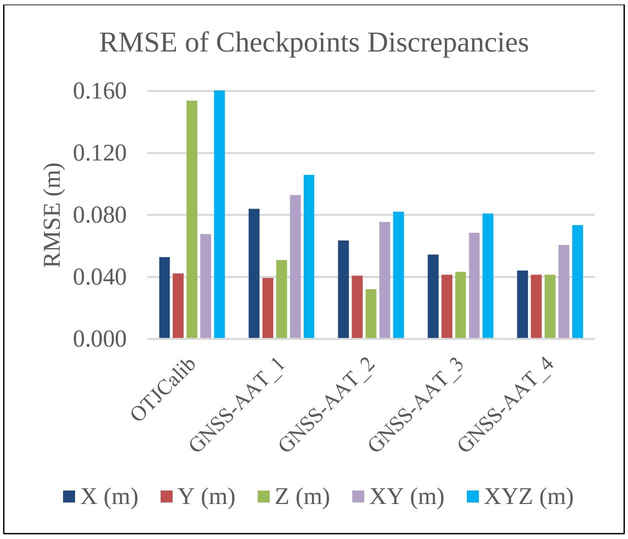

Figure 5. RMSE of discrepancies at checkpoints.

Among the experiments using IOPs from on-site calibration with a sub-block of oblique images (GNSS-AAT 2 to 4), the X RMSEs are slightly worse than the Y and Z RMSE. Notably, in GNSS-AAT_4, which incorporates two sub-blocks of oblique images, the RMSE values for the coordinate's discrepancies are similar, with 0.044 m for X and 0.041 m for both Y and Z. This configuration achieved better horizontal and 3D RMSE values among all the experiments conducted.

When comparing the OTJCalib with four on-site calibration experiments, a notable improvement in vertical accuracy is observed, with up to a 79% increase in GNSS-AAT_2. However, due to more significant errors on the X-axis in GNSS-AAT_1 and GNSS-AAT_2, their horizontal RMSE values are worse than those of OTJCalib. In contrast, GNSS-AAT_3 achieves the same horizontal RMSE (XY) as OTJCalib, with a value of 0.068 m, while GNSS-AAT_4 shows a slightly better result of 0.061 m. Finally, regarding 3D (XYZ) RMSE, all GNSS-AAT experiments improved significantly compared to the on-the-job calibration, reducing 56% of the value of the RMSE XYZ in the GNSS-AAT_4.

5. Discussion

According to the results obtained (Table 3), performing on-site calibration with sub-blocks of images can lead to significant variation in the estimated IOP values compared to the on-the-job calibration of the full corridor block. The results obtained from the two calibrations using only vertical images, OTJCalib and OSCalib_1, are compared, and the focal length difference is 0.013 mm. Using the IOP parameters from OSCalib_1 to perform the GNSS-AAT_1 improved the vertical accuracy 67% compared with the obtained results in the OTJCalib. Although horizontal accuracy decreases in GNSS-AAT_1 due to a bias along the X-axis, the 3D (XYZ) RMSE of checkpoints' discrepancies still shows a 37% improvement compared to OTJCalib, from 4.4 GSD to 2.8 GSD. In the camera calibration, OTJCalib used the entire corridor block of 279 vertical images (3.2 km x 450 m), whereas OSCalib_1 utilized a sub-block of 40 vertical images (750 m x 450 m). Consequently, the RMSE of the checkpoints (Figure 5) suggests that a block with more proportional dimensions can yield a more suitable solution for IOP estimation and improve 3D extraction accuracy. This indicates that, in UAS photogrammetry with SfM-MVS, the block dimension ratio may influence the estimation of an optimal solution for camera calibration. On the other hand, the bias observed on the X-axis, which led to a reduction in horizontal accuracy in GNSS-AAT_1, was unexpected. Thus, a more comprehensive investigation of the correlation between EOPs and IOPs may provide further insight into these results.

Analyzing all the photogrammetric experiments, it can be concluded that adding oblique images for camera calibration results in significant variation in IOP values. Table 3 presents focal length differences of up to 0.020 mm between the on-the-job calibration (OTJCalib) and the on-site calibration experiments OSCalib_3 and OSCalib_4, as well as a variation of up to 22% in the radial distortion parameter k_2 between OTJCalib and OSCalib_2. These results may explain the significant improvement in vertical accuracy, up to 79%, when comparing the RMSE Z values of OTJCalib with GNSS-AAT_2. Checkpoint accuracies (Figure 5) in GNSS-AAT_4 demonstrate that RMSE values close to 1 GSD can be achieved for the three coordinate discrepancies (RMSE X, RMSE Y and RMSE Z) without adding GCPs.

An additional on-the-job calibration experiment was conducted using the block of 279 vertical images with four GCPs (P1, P6, P12, and P17), while the remaining 13 surveyed targets were used as checkpoints. Using four GCPs resulted in checkpoint discrepancies with RMSE X of 0.026 cm (0.7 GSD), RMSE Y of 0.040 cm (1 GSD), and RMSE Z of 0.029 cm (0.7 GSD). Although on-the-job calibration with four GCPs provided greater spatial accuracy than all experiments conducted without GCPs, the RMSE values were similar to those obtained in GNSS-AAT_4. Therefore, in UAS corridor mapping with high-precision GNSS-RTK for direct camera positioning, incorporating oblique image sub-blocks without GCPs can achieve high spatial data acquisition accuracy, close to the accuracy obtained using four Ground Control Points for on-the-job calibration in the analyzed study case.

6. Limitations and Future Work

The outcomes of this study demonstrated the potential of the approach which was studied to improve the accuracy of corridor mapping by UAS photogrammetry without the need for Ground Control Points (GCPs), but using multi-height oblique images and camera station coordinates (X_S, Y_S, Z_S) obtained by the on-board GNSS-RTK sensor. Although the results are promising, future work should investigate more thoroughly the correlation between Exterior and Interior Orientation Parameters (EOPs and IOPs) and residuals in image-space observations to better understand the influence of sub-block geometry on camera calibration. These analyses require further investigation through the Metashape Python API, as they are not directly accessible in the Graphical User Interface (GUI) for end users in version 2.1.2 and were not directly obtainable through the Python console in initial attempts. An analysis of the significance of IOPs estimated under different calibration settings is also recommended.

One limitation of this study is that the proposed methodology was tested in a single study area. Therefore, it is advised to replicate the approach with various instruments (e.g., different cameras and UAV platforms) and to apply it to corridors with different terrain types (e.g., coastal regions with varying elevations and riverbanks with flat terrain) to enhance the robustness and generalizability of the findings.

7. Conclusions

As widely established in photogrammetry literature, including oblique images can enhance the precision of Interior Orientation Parameter (IOP) estimation and, commonly, improve spatial data acquisition accuracy. Nevertheless, to our knowledge, existing studies have not sufficiently explored more feasible methods for incorporating oblique images in corridor blocks, such as utilizing only sub-blocks of multi-height oblique images to improve camera calibration. Therefore, this study aimed to contribute to UAS photogrammetry for corridor mapping with two key contributions: (1) developed a more efficient solution for camera calibration using only sub-blocks of images, without the need for acquiring multi-height and oblique images along the entire corridor block; and (2) achieved significant improvements in vertical accuracy, and thus high-precision spatial data acquisition, without the need for Ground Control Points (GCPs).

To perform this study, four on-site camera calibration experiments were conducted with different configurations of image sub-blocks: (1) 40 vertical images captured at a flight height of 320 m AGL; (2) 40 vertical images + 19 oblique images at an 18° inclination on the Y-axis (pitch), captured at 200 m AGL; (3) 40 vertical images + 21 oblique images at a 45° inclination on the Y-axis (pitch), captured at 200 m AGL; and (4) 40 vertical images + 19 oblique images at an 18° inclination + 21 oblique images at a 45° inclination. One on-the-job calibration experiment using the entire vertical corridor block (279 vertical images) was also performed for comparative purposes. Subsequently, four GNSS-Assisted Aerial Triangulation (GNSS-AAT) experiments were conducted using the entire corridor block, with IOPs fixed according to the corresponding on-site camera calibration.

The outcomes of this study demonstrate that the on-site camera calibration approach using sub-blocks of images can result in significant variations in the estimated focal length values compared to the on-the-job calibration. This variation may account for the substantial improvement in vertical accuracy observed in the four GNSS-AAT experiments, where IOPs derived from the on-site calibration were used. These improvements reduced the RMSE Z values at the checkpoint discrepancies by 67% to 79% compared to the on-the-job calibration experiment.

On the other hand, corridor mapping using direct camera positions measured by onboard GNSS RTK or PPK may still

https://doi.org/10.5194/isprs-annals-X-G-2025-657-2025

require a set of Ground Control Points (GCPs) to achieve geo-information extraction with vertical accuracy below 3 GSD, as shown in the results of Pilartes-Congo *et al.* (2024). However, the outcomes of the present study show that high accuracy in the three coordinates can be achieved without GCPs. The highest accuracy, computed by the RMSE X, Y, and Z checkpoints' discrepancies, was approximately 1 GSD. This accuracy was made possible by using IOPs estimated from the on-site calibrations OSCalib_3 and OSCalib_4 that included oblique sub-blocks. The best results were observed in the GNSS-AAT_4 experiment with a nadir image block and two sub-blocks of oblique images at different inclinations, yielding a 3D (XYZ) RMSE of 1.9 GSD.

Although this study was conducted in a unique test area, the outcomes demonstrate that the proposed methodology significantly improves the accuracy of geospatial data extraction by UAS photogrammetry without the need for GCPs. Therefore, it is strongly recommended that this proposed methodology be applied to different corridor block datasets to validate its effectiveness further.

Acknowledgments

The authors would like to thank the Brazilian governmental agencies CNPq (The National Council for Scientific and Technological Development) for the PhD grant and CAPES (The Coordinating Agency for Advanced Training of High-Level Personnel) for the Institutional Internationalization Program (PrInt) grant, which funded this study.

References

Agisoft, 2024. Agisoft Metashape User Manual: Professional Edition, Version 2.1. agisoft.com/pdf/metashape-pro_2_1_en.pdf.

Andaru, R., Rau, J. Y., Chuang, L. Z. H., Jen, C. H, 2022. Multitemporal UAV photogrammetry for sandbank morphological change analysis: evaluations of camera calibration methods, co-registration strategies, and the reconstructed DSMs. *IEEE Journal of Selected Topics in Applied Earth Observations and Remote Sensing*, *15*, 5924-5942.

Antoine, R., Lopez, T., Tanguy, M., Lissak, C., Gailler, L., Labazuy, P., Fauchard, C., 2020. Geoscientists in the sky: Unmanned aerial vehicles responding to geohazards. *Surveys in Geophysics*, *41*(6), 1285-1321.

Bay, H., Ess, A., Tuytelaars, T., Van Gool, L, 2008. Speeded-up robust features (SURF). *Computer vision and image understanding*, *110*(3), 346-359.

Benjamin, A. R., O'brien, D., Barnes, G., Wilkinson, B. E., Volkmann, W, 2020. Improving data acquisition efficiency: Systematic accuracy evaluation of GNSS-assisted aerial triangulation in UAS operations. *Journal of surveying engineering*, *146*(1), 05019006.

Clédat, E., Cucci, D. A., Skaloud, J., 2020. Camera calibration models and methods for corridor mapping with UAVS. *ISPRS Annals of the Photogrammetry, Remote Sensing and Spatial Information Sciences*, *1*, 231-238.

Costa, F. A., Mitishita, E. A., Martins, M., 2018. The influence of sub-block position on performing integrated sensor orientation using in situ camera calibration and lidar control points. *Remote Sensing*, *10*(2), 260.

Deliry, S. I., Avdan, U., 2021. Accuracy of unmanned aerial systems photogrammetry and structure from motion in surveying and mapping: a review. *Journal of the Indian Society of Remote Sensing*, *49*(8), 1997-2017.

Eltner, A., Baumgart, P., Maas, H. G., Faust, D., 2015. Multi-temporal UAV data for automatic measurement of rill and interrill erosion on loess soil. Earth Surface Processes and Landforms, 40(6), 741-755.

Ferrer-González, E., Agüera-Vega, F., Carvajal-Ramírez, F., Martínez-Carricondo, P., 2020. UAV photogrammetry accuracy assessment for corridor mapping based on the number and distribution of ground control points. *Remote sensing*, *12*(15), 2447.

Forlani, G., Dall'Asta, E., Diotri, F., Morra di Cella, U., Roncella, R., Santise, M., 2018. Quality assessment of DSMs produced from UAV flights georeferenced with on-board RTK positioning. *Remote sensing*, *10*(2), 311.

Goncalves, J. A., Henriques, R., 2015. UAV photogrammetry for topographic monitoring of coastal areas. ISPRS journal of Photogrammetry and Remote Sensing, 104, 101-111.

Habib, A., Kersting, A. P., Bang, K., 2010. Comparative Analysis of Different Approaches for the incorporation of position and orientation information in integrated sensor orientation procedures. In *Proceedings of Canadian Geomatics Conference 2010 and ISPRS Commision I Symposium*.

James, M. R., Robson, S., 2014. Mitigating systematic error in topographic models derived from UAV and ground-based image networks. *Earth Surface Processes and Landforms*, *39*(10), 1413-1420.

La Salandra, M., Colacicco, R., Dellino, P., Capolongo, D., 2023. An effective approach for automatic river features extraction using high-resolution UAV imagery. *Drones*, *7*(2), 70.

Liu, X., Lian, X., Yang, W., Wang, F., Han, Y., Zhang, Y., 2022. Accuracy assessment of a UAV direct georeferencing method and impact of the configuration of ground control points. *Drones*, *6*(2), 30.

Lowe, D. G., 2004. Distinctive image features from scale-invariant keypoints. *International journal of computer vision*, *60*, 91-110.

Luhmann, T., Robson, S., Kyle, S., Harley, I., 2006. *Close range photogrammetry*. Caithness, UK: Wiley Whittles Publishing.

Meinen, B. U., Robinson, D. T., 2020. Streambank topography: An accuracy assessment of UAV-based and traditional 3D reconstructions. *International Journal of Remote Sensing*, *41*(1), 1-18.

Mitishita, E., Barrios, R., Centeno, J., 2014. The influence of the in situ camera calibration for direct georeferencing of aerial imagery. *The International Archives of the Photogrammetry, Remote Sensing and Spatial Information Sciences*, *40*, 273-278.

Nahon, A., Molina, P., Blázquez, M., Simeon, J., Capo, S., Ferrero, C., 2019. Corridor mapping of sandy coastal foredunes with UAS photogrammetry and mobile laser scanning. *Remote Sensing*, *11*(11), 1352.

Pilartes-Congo, J. A., Starek, M. J., Pashaei, M., Berryhill, J., 2024. Examination of UAS-SfM and UAS-Lidar for Survey Repeatability of Roadway Corridors. In *IGARSS 2024-2024 IEEE International Geoscience and Remote Sensing Symposium* (pp. 6605-6608). IEEE.

Pitombeira, K., Mitishita, E., 2023. Influence of On-Site Camera Calibration with Sub-Block of Images on the Accuracy of Spatial Data Obtained by PPK-Based UAS Photogrammetry. *Remote Sensing*, *15*(12), 3126.

Przybilla, H. J., Bäumker, M., Luhmann, T., Hastedt, H., Eilers, M., 2020. Interaction between direct georeferencing, control point configuration and camera self-calibration for RTK-based UAV photogrammetry. *The International Archives of the Photogrammetry, Remote Sensing and Spatial Information Sciences*, *43*, 485-492.

Smith, M. W., Carrivick, J. L., Quincey, D. J., 2016. Structure from motion photogrammetry in physical geography. *Progress in physical geography*, *40*(2), 247-275.

Stöcker, C., Nex, F., Koeva, M., Gerke, M., 2017. Quality assessment of combined IMU/GNSS data for direct georeferencing in the context of UAV-based mapping. *The International Archives of the Photogrammetry, Remote Sensing and Spatial Information Sciences*, *42*, 355-361.

Zhou, Y., Rupnik, E., Meynard, C., Thom, C., Pierrot-Deseilligny, M, 2019. Simulation and analysis of photogrammetric UAV image blocks—Influence of camera calibration error. *Remote Sensing*, *12*(1), 22.